



Chemical Reaction and Soret Effects on MHD Free Convection Flow Past a Vertical Porous Plate with Heat Generation

M. Dhanalakshmi¹, K. Jayarami Reddy^{1*}, K. Ramakrishna²

¹Department of Mathematics, K. L. University, Guntur-522502. India

²Mechanical Engineering, K. L. University, Guntur-522502. India

Abstract: This paper deals with the chemical reaction and soret effect of heat generation on the MHD free convection heat and mass transfer flow of a viscous incompressible fluid past a continuously moving infinite plate including thermal radiation. Closed form of solution for the velocity, temperature and concentration field are obtained and discussed graphically for various values of the physical parameters present. In addition, expressions for the skin friction and Sherwood number is also derived and finally discussed with the graphs.

Keywords: Free convection, Heat Generation, Magnetic Field, chemical reaction, porous plate, Soret effect, Thermal radiation.

Introduction:

The study of convective heat and mass transfer fluid flow over stretching surface in the presence of thermal radiation, heat generation and chemical reaction is gaining a lot of attention. This study has many applications in industries, many engineering disciplines. These flows occur in many manufacturing processes in modern industry, such as hot rolling, hot extrusion, wire drawing and continuous casting. For example, in many metallurgical processes such as drawing of continuous filaments through quiescent fluids and annealing and tinning of copper wires, the properties of the end product depends greatly on the rate of cooling involved in these processes. The free convection flow of a viscous incompressible electrically conducting fluid through the channel in the presence of a transverse magnetic field has important applications in magnetohydrodynamic generators, pumps, accelerators, cooling systems, centrifugal separation of matter from fluid, petroleum industry, purification of crude oil, electrostatic precipitation, polymer technology and fluid droplets sprays etc. The performance and efficiency of these devices are influenced by the presence of suspended solid particles in the wear activities and/or the combustion processes in MHD generators and plasma MHD accelerators. The study of Magnetohydrodynamics flow for an electrically conducting fluid past a heated surface has attracted the interest of many researchers in view of its important applications in many engineering problems such as plasma studies, petroleum industries. MHD power generators, cooling of nuclear reactors, The MHD fluid flow in a parallel plate channel is an interesting area in the study of fluid mechanics because of its relevance to various engineering applications.

Flow of an incompressible viscous fluid over a stretching surface is a classical problem in fluid dynamics and important in various process. It is used to create polymers of fixed cross-sectional profiles, cooling of metallic and glass plates. Aerodynamics shaping of plastic sheet by forcing through die and boundary layer along a liquid film in condensation processes are among the other areas of application. The production of sheeting material, which includes both metal and polymer sheets arises in a number of industrial manufacturing processes. Chamkha [1] studied the effect of heat generation/absorption in MHD flow of

uniformly stretched vertical permeable surface in presence of chemical reaction. Vidyasagar [2] have investigated radiation and chemical reaction effects on MHD free convection flow of a uniformly vertical porous plate with heat source. The effect of radiation on heat transfer problems have been studied by Hossain and Takhar [3]. Seddeek [4] analyzed the effects of radiation and variable viscosity on a MHD free convection flow past a semi-infinite flat plate with an aligned magnetic field. In many chemical engineering processes, chemical reactions take place between a foreign mass and the working fluid which moves due to the stretch of a surface.

Kandasamy [5] analyzed effects of chemical reaction, heat and mass transfer on boundary layer flow over a porous wedge with heat radiation in the presence of suction or injection. Muhaimin [6] studied the effect of chemical reaction, heat and mass transfer on nonlinear MHD boundary layer past a porous shrinking sheet with suction. Rajesh [7] investigated chemical reaction and radiation effects on the transient MHD free convection flow of dissipative fluid past an infinite vertical porous plate with ramped wall temperature. Renuka [8] studied the Soret effect on unsteady MHD free convective mass transfer flow past an infinite vertical porous plate with variable suction. Vidyasagar and Ramana [9] studied thermal diffusion effect on MHD free convection heat and mass transfer flow past a uniformly vertical plate with heat sink. Sarada and Shanker [10] analyzed the effect of thermal radiation on an unsteady MHD flow past vertical porous heated plate with chemical reaction and viscous dissipation. Sharma [11] discussed unsteady MHD free convective flow and heat transfer between heated inclined plates with magnetic field in the presence of radiation effects. Mohan Krishna [12] investigated Soret and Dufour Effects on MHD Free Convective Flow over a Permeable Stretching Surface with Chemical Reaction and Heat Source. Srinivasa Rao [13] studied effect of thermal radiation on MHD boundary layer flow over a moving vertical porous plate with suction. Abdul Gaffar [14] studied thermal radiation and heat generation/absorption effects on viscoelastic double-diffusive convection from an isothermal sphere in porous media. Rafael Cortell [15] investigated Internal Heat Generation and Radiation Effects on a Certain Free Convection Flow.

The objective of the present study is to investigate the effects of thermal diffusion and heat absorption on two-dimensional free convection mass transfer flow past a vertical porous plate in the presents of chemical reaction. The velocity, temperature and concentration field are obtained and discussed graphically for various values of the physical parameters present. In addition, expressions for the skin friction and Sherwood number is also derived and finally discussed through the graphs.

Mathematical Formulation

We consider a steady laminar flow of a viscous incompressible fluid past an infinite vertical porous flat plate. Introduce a coordinate system (x, y) with x -axis along the length of the plate in the upward vertical direction and y -axis normal to the plate towards the fluid region. The plate is subjected to a constant suction parallel to y -axis. The viscous dissipations of energy are assumed to be negligible for the study. Since, the plate is infinite in length all the fluid property except possibly the pressure remain constant along the x -direction. The fluid property variation with temperature is limited to density variation only and the influence of variation of density with temperature is restricted to the body force term only, in accordance with the Boussinesq approximation. Under boundary layer and Boussinesq approximations, the equations governing the steady laminar two dimensional free convective flow with medium concentration in presence of Soret and Chemical reaction effects reduce to:

Continuity Equation:

$$\frac{\partial \bar{v}}{\partial y} = 0 \quad (1)$$

Momentum Equation:

$$\bar{v} \frac{\partial \bar{u}}{\partial y} = \nu \frac{\partial^2 \bar{u}}{\partial y^2} + g\beta(\bar{T} - \bar{T}_\infty) + g\beta^*(\bar{C} - \bar{C}_\infty) - \frac{\sigma B_o^2}{\rho} \bar{u} - \frac{\nu}{k^*} \bar{u} \quad (2)$$

Energy Equation:

$$\bar{v} \frac{\partial \bar{T}}{\partial y} = \frac{k}{\rho c_p} \frac{\partial^2 \bar{T}}{\partial y^2} - \frac{1}{\rho c_p} \frac{\partial q_r}{\partial y} + \frac{Q_o}{\rho c_p} (\bar{T} - \bar{T}_\infty) \tag{3}$$

Species Concentration

$$\bar{v} \frac{\partial \bar{C}}{\partial y} = D_M \frac{\partial^2 \bar{C}}{\partial y^2} + D_T \frac{\partial^2 \bar{T}}{\partial y^2} + K_1 (\bar{C} - \bar{C}_\infty) \tag{4}$$

The boundary conditions are

$$\left. \begin{aligned} \bar{u} = \bar{U}, \bar{v} = -V_o (V_o > 0), \bar{T} = \bar{T}_w, \bar{C} = \bar{C}_w \quad \text{at } \bar{y} \rightarrow 0 \\ \bar{u} \rightarrow 0, \bar{v} \rightarrow -V_o, \bar{T} \rightarrow \bar{T}_\infty, \bar{C} \rightarrow \bar{C}_\infty \quad \text{at } \bar{y} \rightarrow \infty \end{aligned} \right\} \tag{5}$$

We introduce the following non-dimensional quantities as

$$\begin{aligned} y = \frac{V_o \bar{y}}{v}, u = \frac{\bar{u}}{V_o}, U_0 = \frac{\bar{U}}{V_o}, v = \frac{\bar{v}}{V_o}, \theta = \frac{\bar{T} - \bar{T}_\infty}{\bar{T}_w - \bar{T}_\infty}, \phi = \frac{\bar{C} - \bar{C}_\infty}{\bar{C}_w - \bar{C}_\infty} \\ Gr = \frac{g \beta v (\bar{T}_w - \bar{T}_\infty)}{V_o^3}, Gc = \frac{g \beta^* v (\bar{C}_w - \bar{C}_\infty)}{V_o^3}, Pr = \frac{v^2 \rho c_p}{k}, K = \frac{v^2 V_o}{k^*} \\ R = \frac{4 \alpha^2 v}{\rho c_p}, Q = \frac{Q_o v}{\rho c_p}, Sc = \frac{v}{D_M}, Sr = \frac{D_T (\bar{T}_w - \bar{T}_\infty)}{v^2 (\bar{C}_w - \bar{C}_\infty)}, M = \frac{\sigma B_o^2 v}{\rho V_o^2}, \epsilon = \frac{K_1 v}{V_o^2} \end{aligned} \tag{6}$$

The non-dimensional forms of equations are

$$\frac{\partial v}{\partial y} = 0 \tag{7}$$

$$\frac{\partial^2 u}{\partial y^2} + \frac{\partial u}{\partial y} - (M + K)u = -Gr\theta - Gc\phi \tag{8}$$

$$\frac{\partial^2 \theta}{\partial y^2} + Pr \frac{\partial \theta}{\partial y} - Pr(R + Q)\theta = 0 \tag{9}$$

$$\frac{\partial^2 \phi}{\partial y^2} + Sc \frac{\partial \phi}{\partial y} + \epsilon Sc\phi - ScSr \frac{\partial^2 \theta}{\partial y^2} \tag{10}$$

The corresponding non- dimensional boundary conditions are

$$\left. \begin{aligned} u = U_0, v = -1, \theta = 1, \phi = 1, \quad \text{at } y = 0 \\ u \rightarrow 0, v \rightarrow -1, \theta \rightarrow 0, \phi \rightarrow 0, \text{at } y \rightarrow \infty \end{aligned} \right\} = \tag{11}$$

The solutions of equations (8), (9) and (10) are

$$u(y) = U_0 e^{-A_5 y} - A_9 e^{-A_5 y} + A_{10} e^{-A_1 y} + A_6 e^{-A_2 y} \tag{12}$$

$$\theta = e^{-A_1 y}$$

$$\phi = A_4 e^{-A_2 y} - A_3 e^{-A_1 y} \tag{13}$$

where

$$A_1 = \frac{Pr + \sqrt{Pr^2 + 4Pr(R + Q)}}{2}, \quad A_2 = \frac{Sc + \sqrt{Sc^2 - 4CSc}}{2}$$

$$A_3 = \frac{ScSrA_1^2}{A_1^2 - ScA_1 + CSc}, \quad A_4 = 1 + A_3, \quad A_5 = \frac{1 + \sqrt{1 + 4(M + K)}}{2}$$

$$A_6 = \frac{GcA_4}{A_1^2 - A_1 - (M + K)}, \quad A_7 = \frac{Gr}{A_1^2 - A_1 - (M + K)},$$

$$A_8 = \frac{GcA_3}{A_1^2 - A_1 - (M + K)}, \quad A_9 = A_6 - A_{10} = A_{10} - A_7$$

Skin Friction at the plate

The non- dimensional skin friction at the plate is

$$\tau = \left(\frac{\partial u}{\partial y} \right)_{y=0} = A_5 A_9 - A_1 A_{10} - A_2 A_6 - U_0 A_5$$

Sherwood number

The non-dimensional Sherwood number at the plate is

$$Sh = \left(\frac{\partial \phi}{\partial y} \right)_{y=0} = A_1 A_3 - A_2 A_4$$

3. Result and Discussion

Numerical computations have been carried out for different values of Grashof number (Gr), Magnetic Parameter (M), Thermal radiation (R), Permeability parameter (K) Modified Grashof Number (Gc), Heat Source Parameter (Q), Prandtl number (Pr), Schmidt number (Sc), Chemical Parameter (C) and Soret number (Sr). The above mentioned flow parameters, the results are displayed in Figures 1-10 in terms of the concentration, temperature and velocity profiles.

Fig (1) shows that the variation of concentration for different values of chemical reaction Parameter (C). From this figure, we notice that the concentration decreases with the increase of chemical reaction parameter (C). The variation of concentration for different values of Prandtl Number (Pr) are shown in fig (2). From this figure, we notice that the concentration increases with the increase of Prandtl number (Pr). From fig (3) shows that the variation of concentration for different values of heat source parameter (Q). It is observed that the concentration increases with the increase of heat source parameter (Q). The concentration for different values of Schmidt number (Sc) is shown in fig (4). We observe that the Schmidt number (Sc) increases with the decrease of concentration. Fig (5) shows that the variation of concentration for different values of Soret number (Sr). We notice that the concentration increases with the decrease of Soret number (Sr).

The temperature profile for different values of Prandtl number (Pr) is shown in fig (6). It is noticed that the temperature decreases with the increase of Prandtl number (Pr). The variation of temperature for different values of heat source parameter (Q) is shown in fig (7). We observe that the temperature decreases with the increase of heat source parameter (Q). From fig (8) shows that the variation of temperature for different values of radiation parameter (R). We notice that the temperature decreases with the increase of radiation parameter (R).

From fig (9) shows that the variation of velocity for different values of Chemical Reaction (Ch). We observe that the velocity decreases with the increase of Chemical Reaction (Ch). The variation of velocity for different values of Grashof number (Gr) is shown in fig (10). It is observed that the velocity increases with the increase of Grashof number (Gr). The variation of velocity for different values of permeability parameter (K) is

shown in fig (11). We notice that the velocity decreases with the increase of Permeability parameter (K). From fig (12) shows that the variation of velocity for different values of magnetic parameter (M). It is observe that the velocity decreases with the increase of magnetic parameter (M). The variation of velocity for different values of Prandtl number (Pr) is shown in fig (13). We notice that the velocity increases with the increase of Prandtl number (Pr). From fig (14) shows that the variation of velocity for different values of Heat generation (Q). It is observe that the velocity increases with the increase of Heat generation (Q). From fig (15) shows that the variation of velocity for different values of Schmidt number (Sc). It is observe that the velocity decreases with the increase of Schmidt number (Sc). The variation of velocity for different values of Soret number (Sr) is shown in fig (16). We notice that the velocity decreases with the increase of Soret number (Sr).

The Sherwood for different values of Chemical Reaction (Ch) is shown in fig (17). We notice that the Sherwood increases with the increase of Chemical Reaction (Ch), but it takes the reverse action. The Sherwood for different values of Schmidt number (Sc) is shown in fig (17). We notice that the Sherwood decreases with the increase of Schmidt number (Sc), but it takes the reverse action. The Skin-Friction for different values of Permeability Parameter (K) is shown in fig (19). It is observe that the Skin-friction decreases with the increase Permeability Parameter (K). The Skin-Friction for different values of Chemical Reaction (Ch) is shown in fig (20). We observe that the Skin-friction increases with the increase of Chemical Reaction (Ch). The Skin-Friction for different values of magnetic parameter (M) is shown in fig (21). We notice that the Skin-friction increases with the increase of magnetic parameter (M). The Skin-Friction for different values of radiation parameter (R) is shown in fig (22). It is observed that the Skin-friction decreases with the increase of radiation parameter (R).

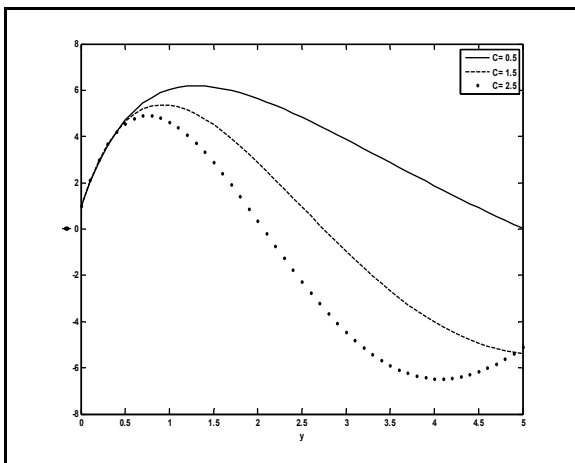


Fig (1): The concentration profile for different values of C

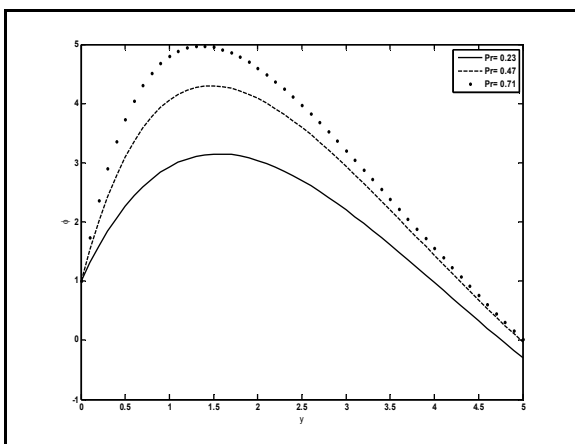


Fig (2): The concentration profile for different values of Pr

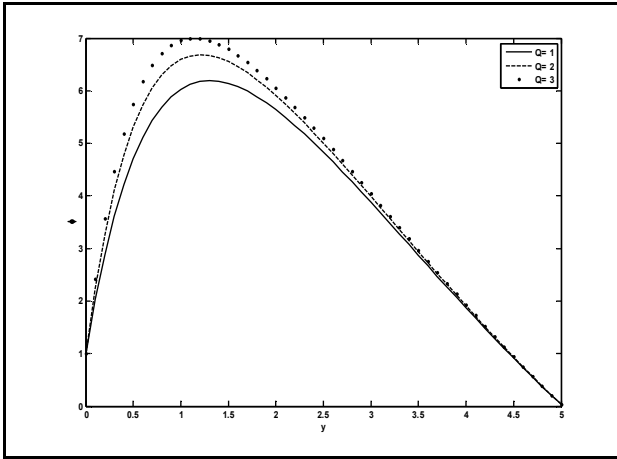


Fig (3): The concentration profile for different values of Q

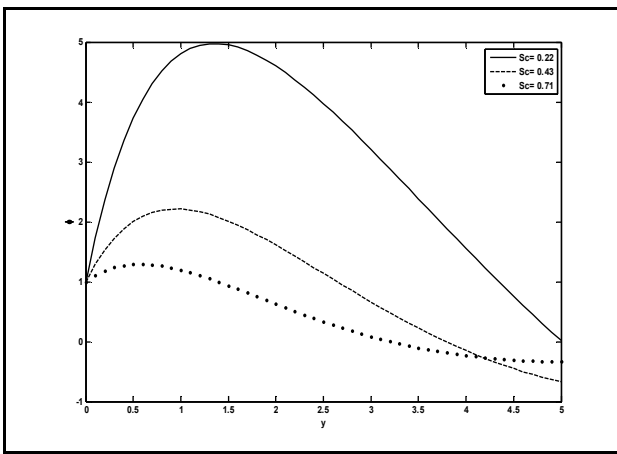


Fig (4): The concentration profile for different values of Sc

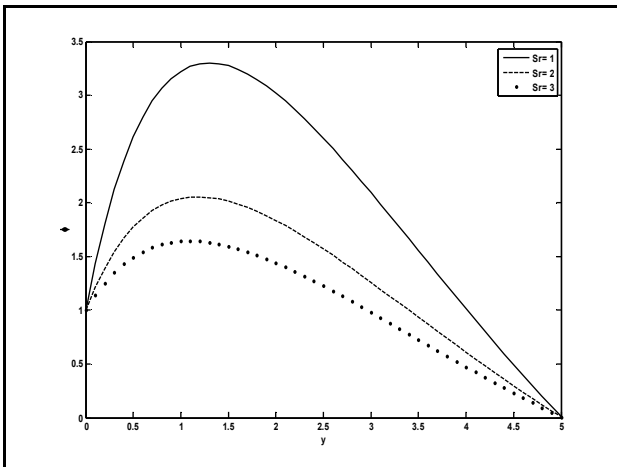


Fig (5): The concentration profile for different values of Sr

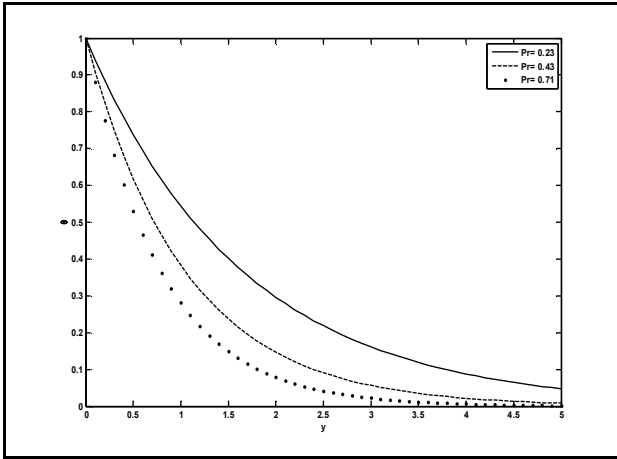


Fig (6): The temperature profile for different values of Pr

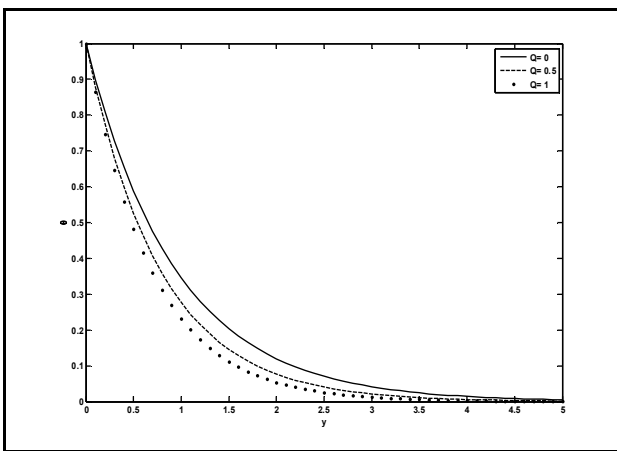


Fig (7): The temperature profile for different values of Q

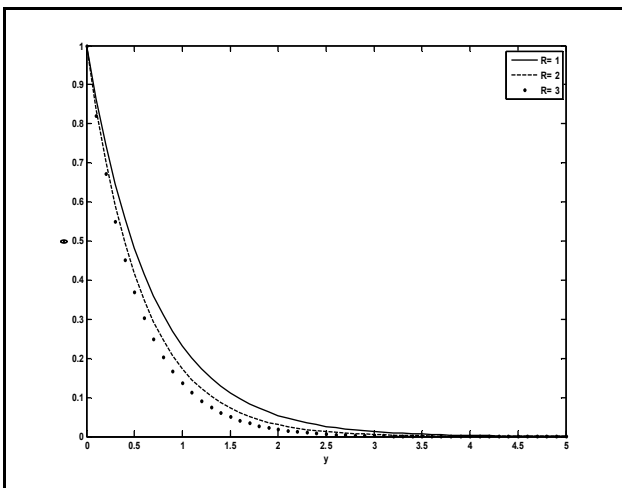


Fig (8): The temperature profile for different values of R

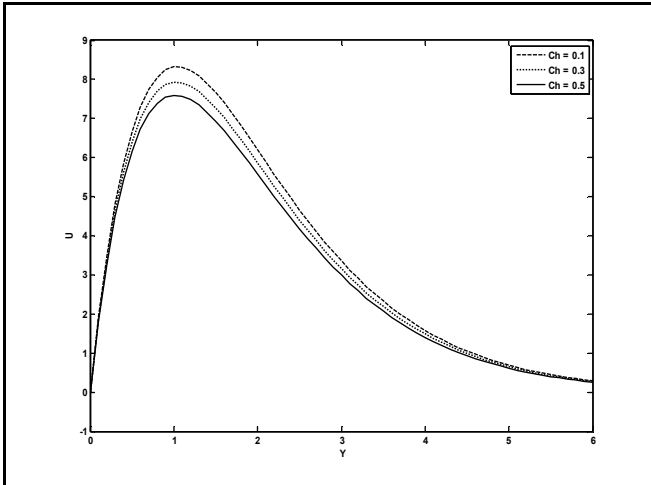


Fig (9): The velocity profile for different values of Ch

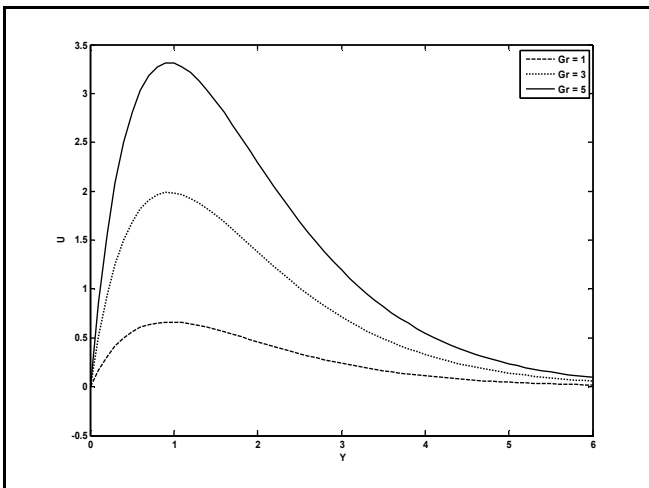


Fig (10): The velocity profile for different values of Gr

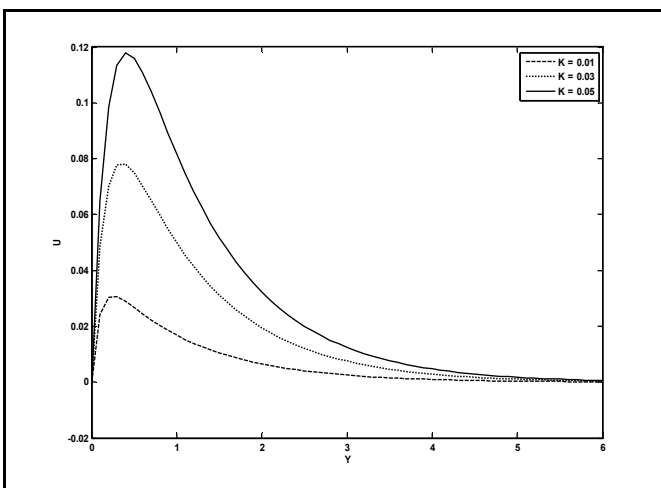


Fig (11): The velocity profile for different values of K

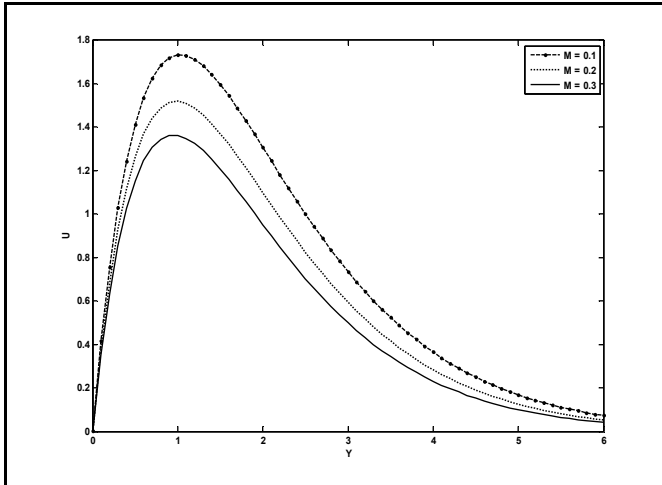


Fig (12): The velocity profile for different values of M

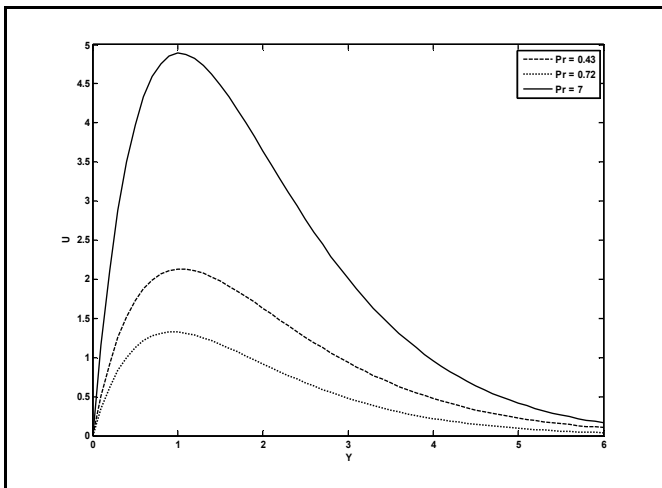


Fig (13): The velocity profile for different values of Pr

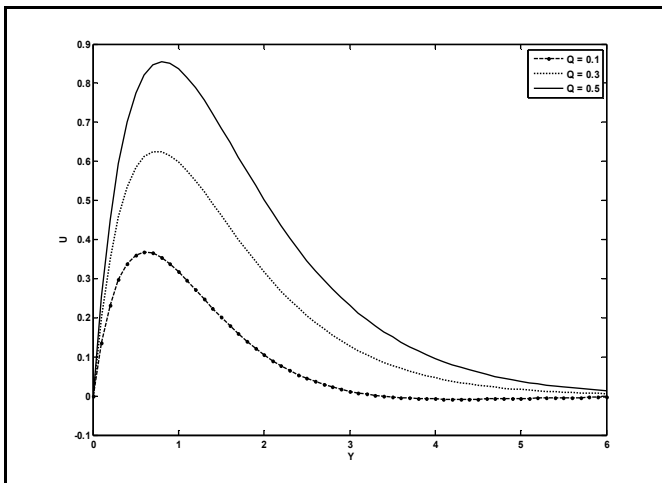


Fig (14): The velocity profile for different values of Q

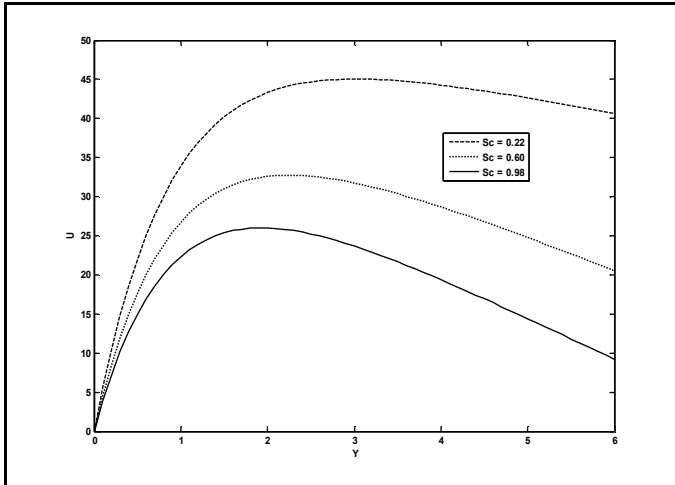


Fig (15): The velocity profile for different values of Sc

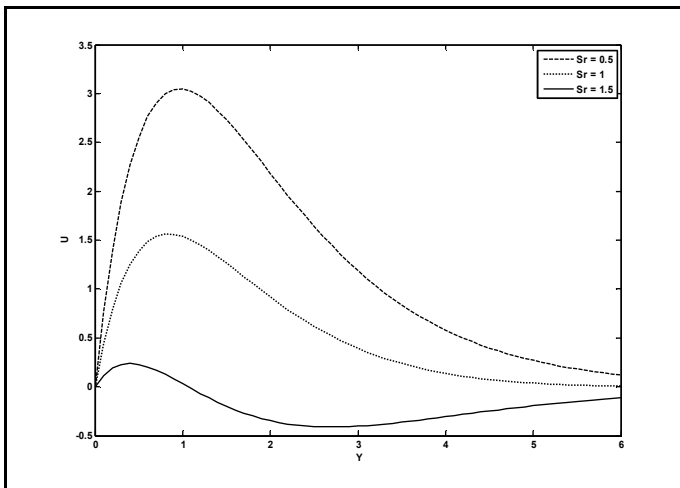


Fig (16): The velocity profile for different values of Sr

Table 1: Numerical values of the Skin-friction coefficient (C_f), for M, K, Pr, Ra, Gr, Gc, Sc, Sr, Ch, Q.

Pr	M	Gr	Gc	K	Ra	Ch	Sr	Sc	Q	C_f
0.72	3	1	3	1	3	0.5	0.6	0.22	1	1.879912
0.72	3	5	3	1	3	0.5	0.6	0.22	1	-9.034211
0.72	5	1	3	1	3	0.5	0.6	0.22	1	-6.546651
0.72	3	1	5	1	3	0.5	0.6	0.22	1	-11.868342
0.72	3	1	3	5	3	0.5	0.6	0.22	1	-5.936872
0.72	3	1	3	1	5	0.5	0.6	0.22	1	-33.835061
0.72	3	1	3	1	3	0.3	0.6	0.22	1	-9.230912
0.72	3	1	3	1	3	0.5	0.6	1.6	1	1.879912
7	3	1	3	1	3	0.5	0.6	0.22	1	-2.368174
0.72	3	1	3	1	3	0.5	0.43	0.22	1	-9.394596
0.72	3	1	3	1	3	0.5	0.6	0.22	5	9.489755

Table 2: Numerical values of the Sherwood (Sh), for M, K, Pr, Ra, Gr, Gc, Sc, Sr, Ch, Q.

Pr	M	Gr	Gc	K	Ra	Ch	Sr	Sc	Q	Sh
0.72	3	1	3	1	3	0.5	0.43	0.22	1	0.094081
0.72	3	1	3	1	3	0.5	0.6	1.6	1	2.170087
7	3	1	3	1	3	0.5	0.6	0.22	1	1.202774
0.72	5	1	3	1	3	0.5	0.6	0.22	1	0.172381

0.72	3	1	3	1	1	0.5	0.6	0.22	1	0.106992
0.72	3	1	3	1	3	0.3	0.6	0.22	1	0.225207
0.72	3	1	3	1	3	0.5	0.6	0.22	1	0.264837
0.72	3	1	3	1	3	0.5	0.6	0.22	3	0.222559
0.72	3	3	3	1	3	0.5	0.6	0.22	1	0.222549
0.72	3	1	1	1	3	0.5	0.6	0.22	1	0.222569

5. Conclusion

In this Paper we discuss the radiation and chemical reaction effects on MHD free convection flow of a uniformly vertical porous plate with heat generation. The expressions for the velocity, temperature and concentration distributions are the equations governing the flow are numerically solved by perturbation technique.

- The velocity increases with the increase of permeability parameter K .
- The temperature decreases with the increase of radiation parameter R .
- The concentration decreases with the increase of chemical reaction parameter C .
- The Sherwood increases with the increase of Chemical Reaction (Ch), but it takes the reverse action.
- The Sherwood decreases with the increase of Schmidt number (Sc), but it takes the reverse action.
- The Skin-friction increases with the increase Permeability Parameter (K).
- The Skin-friction decreases with the increase of Chemical Reaction (Ch).

6. References:

1. Chamkha, A. J., Int. Comm. Heat Mass Transfer, 2003,30, 413–22.
2. Vidyasagar, G., Ramana, B., and Mohan Krishna, P., Int. J. of Scientific & Engg Research, 2015, 6 (9), 223-227.
3. Takhar, H. S., Gorla R. S. R., and Soundalgekar, V. M., Int. J N. Meth Heat Fluid Flow, 1996, 6, 77-83.
4. Seddeek, M. A., Int. J. Heat Mass Transfer, 2002, 45, 931-935.
5. Kandasamy, R., Wahid, B., Md. Raj, and Azme B. Khamis, Theoret. Appl. Mech., 2006, 33 (2), 123.
6. Muhaimin, Ramasamy Kandasamy, I. Hashim and Azme B. Khamis, Theoret. Appl. Mech., 2009, 36 (2), 101-117.
7. Rajesh, V., Chemical Industry & Chemical Engineering Quarterly, 2011, 17 (2), 189-198.
8. Renuka, S., Krishna, N. , Rao, J., and Anand, Int. J. of Petroleum Sci. and Techn., 2009, 3, 43-50.
9. Vidyasagar, G., and Ramana, B., Journal of Global Research in Mathematical Archives, 2013, 1(2), 41-48.
10. Sarada K & Shanker B, Int. J. of Mathematical Archive, 2013, 4(5), 296-310.
11. Sharma P. R, Navin Kumar and Pooja Sharma, J. Int. Academy of Phy. Sci., 2010, 14 (2), 181-193.
12. Mohan Krishna, P., Vidyasagar, G., Sandeep, N., and Sugunamma, V., Int. J. Scientific & Engg. Research, 2015, 6 (9), 243-247.
13. Srinivasa Rao, G., Ramana, B., Rami Reddy, B., and Vidyasagar, G., Int. J. Math. Archive, 2014, 5(4), 169-181.
14. Abdul Gaffar, S., Ramachandra Prasad, V., Keshava Reddy, E., and Anwar Béq, O., Ain Shams Engg. J., 2015, 6, 1009–1030.
15. Rafael Cortell, Int. J. Nonlinear Science, 2010, 9 (4), 468-479.
